https://doi.org/10.5194/egusphere-2026-4504
Preprint. Discussion started: 3 September 2026

Anthropogenic-biogenic interactions and regional transport drive summer ozone formation in an agricultural-urban interface of Northeast China

Xinpeng Ye[1, a], Qian Jiang[2, 3, a], Jin Ban[1], Mengyu Xie[4], Qianyi Xu[1], Zeyu Wang[1], Jian Sun[1*], Hongai Zhang[5], Xinyi Niu[6], Hongmei Xu[1], Zhenxing Shen[1], Guohui Li[3]

[1]*Department of Environmental Science and Engineering, Xi'an Jiaotong University, Xi'an 710049, China*

[2]*School of Environmental Science and Engineering, Southwest Jiaotong University, Chengdu, 611756, Sichuan, China.*

[3]*Key Lab of Aerosol Chemistry & Physics, SKLLQG, Institute of Earth Environment, Chinese Academy of Sciences, Xi'an 710049, China*

[4]*East China University of Science and Technology, Shanghai 200237, China*

[5]*Department of Neonatology, Shanghai General Hospital Affiliated to Shanghai Jiao Tong University School of Medicine, 650 Xinsongjiang Rd, Songjiang District, Shanghai 201620, China*

[6]*Department of Occupational and Environmental Health, School of Public Health, Xi'an Jiaotong University Health Science Center, Xi'an 710049, China*

[a]*These authors contributed equally to this work and should be considered as co-first authors.*

**Author to whom correspondence should be addressed. E-mail: sunjian0306@mail.xjtu.edu.cn (Jian Sun).*

https://doi.org/10.5194/egusphere-2026-4504
Preprint. Discussion started: 3 September 2026

Abstract

Agricultural-urban interfaces (AUIs) present distinct photochemical environments shaped by the intense mixing of anthropogenic and biogenic precursors. To elucidate the mechanisms driving summer ozone (O_3) formation in these regions, we conducted an integrated study in Siping, a representative AUI in Northeast China, utilizing high-time-resolution volatile organic compound (VOC) observations (2021-2022), positive matrix factorization (PMF), and Weather Research and Forecasting model coupled with Chemistry (WRF-Chem) simulations. Observational data indicated that while alkanes and oxygenated VOCs dictate atmospheric abundances, the O_3 formation potential is primarily governed by reactive alkenes and biogenic isoprene. PMF source apportionment identified vehicle exhaust (56.4%) and biogenic emissions from crops and vegetation as critical VOC sources. However, WRF-Chem modeling revealed a pronounced decoupling between local VOC source contributions and actual O_3 production. Regional transport and background concentrations collectively account for nearly 90% of the ambient O_3 burden, significantly dwarfing local photochemical production. Empirical kinetic modeling approach (EKMA) analysis showed that local O_3 formation operates within a transition regime sensitive to both VOCs and NO_x. Although regional transport dominates the overall O_3 inventory, scenario simulations demonstrate that mitigating biogenic emissions is unfeasible as a natural source, and industrial emission controls yield negligible benefits due to suboptimal VOC/NO_x emission ratios. Consequently, controlling local transportation emissions emerges as the most viable and practically effective pathway to alleviate O_3 pollution in AUIs. This study provides a quantitative basis for formulating O_3 mitigation strategies in complex agricultural-urban environments, emphasizing the necessity of integrating regional joint control with targeted local vehicle emission reductions.

Keywords: Agricultural-urban interface, ozone formation sensitivity, VOC source apportionment, regional transportation, ozone formulation

https://doi.org/10.5194/egusphere-2026-4504
Preprint. Discussion started: 3 September 2026

Graphic abstract

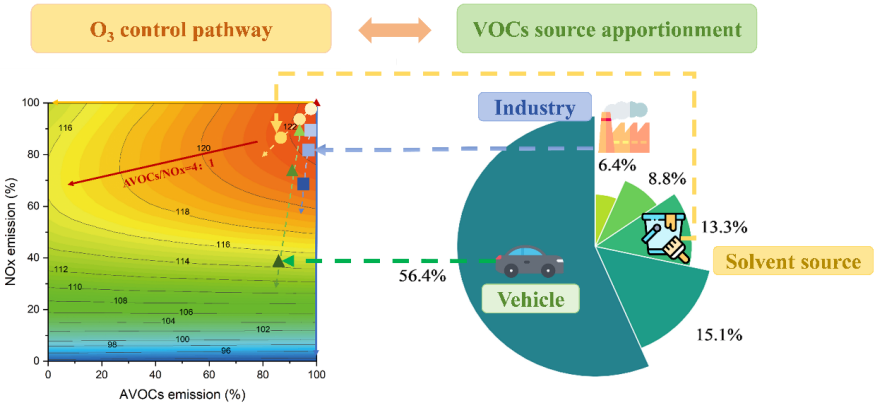

https://doi.org/10.5194/egusphere-2026-4504
Preprint. Discussion started: 3 September 2026

1 Introduction

In recent years, despite continued reductions in primary pollutant emissions worldwide, summertime surface ozone (O_3) pollution has shown an increasing trend across many regions of the world (Wang et al., 2025). As a highly oxidative secondary pollutant, ozone not only poses a serious threat to human respiratory health but also substantially suppresses crop growth, making it a critical risk factor that constrains global food security and ecosystem services (Zhang et al., 2019; Manisalidis et al., 2020). While integrated air pollution control has begun to achieve measurable success in traditional industrialized metropolitan clusters, such as the Beijing-Tianjin-Hebei and Yangtze River Delta regions, the Agricultural-Urban Interface (AUI) is emerging as new hotspots of regional ozone pollution worldwide. This shift is largely driven by rapid urbanization and intensive agricultural activities in these widely distributed transitional regions (Benka-Coker et al., 2020).

Ozone formation is inherently nonlinear and is jointly governed by multiple factors, including volatile organic compounds (VOCs) composition, precursor concentrations (e.g., VOCs and NO_x), meteorological conditions, and regional transport (Zhao et al., 2025; Tao et al., 2024; Wang et al., 2023a). Unlike heavily industrialized or highly urbanized regions, AUIs exhibit a unique physicochemical environment shaped by their distinctive precursor emission profiles. During summer, vigorous crop growth and emissions from agricultural shelterbelts release substantial amounts of highly reactive biogenic volatile organic compounds (BVOCs), particularly isoprene (Cao et al., 2022); At the same time, seasonal agricultural machinery operations, which generate high NO_x emissions, together with potential biomass burning, dispersed agro-industrial activities, and transit traffic, create a highly complex mixture of anthropogenic and natural emission sources. The strong interaction between highly reactive BVOCs and diverse anthropogenic precursors profoundly alters the local RO_x radical cycling, leading to pronounced nonlinearities in ozone production efficiency and precursor sensitivity across the region (Masui et al., 2023; Liu et al., 2026).

Accurately characterizing ozone formation under such a complex emission environment remains a major challenge in atmospheric chemistry. Receptor models

https://doi.org/10.5194/egusphere-2026-4504
Preprint. Discussion started: 3 September 2026

based on high-frequency observations, such as positive matrix factorization (PMF), can effectively identify local VOC sources and quantify their contributions. However, they cannot disentangle the influences of evolving meteorological conditions and large-scale regional transport (Ye et al., 2025); In contrast, three-dimensional chemical transport models, such as Weather Research and Forecasting model coupled with Chemistry (WRF-Chem), can explicitly represent meteorology-chemistry interactions and transport processes. Their performance in agriculturally dominated regions, however, is often constrained by substantial uncertainties in localized emission inventories (Zhang et al., 2026; Gupta et al., 2024).

As one of the world's three major black soil regions and a globally important agricultural hub, the Northeast China Plain provides an ideal natural laboratory for investigating the photochemical mechanisms of O_3 formation in AUI. During summer, the region is characterized by intense solar radiation, open plain wind fields, and a distinctive landscape in which urban areas are embedded within vast agricultural lands. Nevertheless, studies integrating high-resolution field observations with three-dimensional chemical transport modeling remain scarce in this representative region. In particular, quantitative understanding of the coupled effects of local anthropogenic-natural interactions and large-scale regional transport on O_3 formation is still lacking.

To address these knowledge gaps, this study selected Siping, a representative agricultural hub in Northeast China, as the receptor site and established an integrated analytical framework combining high-time-resolution VOC observations, PMF source apportionment, high-resolution WRF-Chem simulations, and empirical kinetic modeling approach (EKMA). The study aims to address three key scientific questions. First, it identifies the key reactive species within the complex precursor mixture of AUI and quantifies the relative contributions of anthropogenic and biogenic emissions to photochemical processes. Second, it quantitatively disentangles the individual and synergistic contributions of local multi-source emissions and large-scale regional transport to summertime O_3 pollution. Third, it explores potential O_3 control pathways by constructing nonlinear O_3-precursor response surfaces specific to agricultural cities.

https://doi.org/10.5194/egusphere-2026-4504
Preprint. Discussion started: 3 September 2026

The findings provide a scientific basis for mitigating complex air pollution in Northeast China. More importantly, the identified mechanisms linking anthropogenic-natural interactions with regional transport offer broader insights into the management of photochemical air pollution in agricultural-urban regions with similar characteristics worldwide.

2 Method

2.1 Study area, sampling, and analytical methods

Siping city (42°31′-44°09′ N, 123°17′-125°49′ E) is located in Northeast China and represents a typical AUI. In 2024, the city had a grain cultivation area of 589,000 ha and a total grain production of 4.901 million tons, reflecting the intensive agricultural activities surrounding the urban area (Statistics Bureau of Jilin, https://tjj.jl.gov.cn/). Ambient measurements were conducted at the Yishangchang National Ambient Air Quality Monitoring Station in central Siping (Fig. S1). No major industrial point sources are located in the immediate vicinity of the site.

VOC measurements were conducted during the high-O_3 season in 2021 and 2022. Ambient air was collected into 3.2 L SUMMA canisters with passivated inner surfaces. Each canister was connected to a 3 h integrated sampler, which served as the sampling inlet and controlled the transfer of ambient air into the canister. Field measurements were carried out primarily under clear or partly cloudy conditions on 14 non-consecutive days from 17 July to 30 August 2021 and on another 14 non-consecutive days from 8 June to 22 July 2022.

To characterize VOC variations under different emission and photochemical conditions, samples were collected during three periods: 08:00-09:00, when anthropogenic emissions were enhanced but photochemical activity remained relatively weak; 14:00-15:00, corresponding to stronger anthropogenic emissions and photochemical activity; and 19:00-20:00, representing relatively low anthropogenic emissions with negligible photochemical activity. In total, 85 samples were obtained, including one field blank. A total of 106 VOC species were quantified and grouped into alkanes, alkenes, alkynes, aromatics, halocarbons, and oxygenated volatile

https://doi.org/10.5194/egusphere-2026-4504
Preprint. Discussion started: 3 September 2026

organic compounds (OVOCs). Further information on chemical analysis and the complete list of measured species is provided in Text S1 and Table S1.

2.2 Ozone formation potential

The photochemical importance of individual VOC species was evaluated using the ozone formation potential (OFP), based on their measured concentrations and corresponding maximum incremental reactivity (MIR) coefficients(Carter, 1994; Zhang et al., 2021; Sha et al., 2021):

$$OFP_i = VOC_i \times MIR_i$$

where OFP_i is the ozone formation potential of VOC species i, VOC_i is its measured concentration, and MIR_i is the corresponding maximum incremental reactivity coefficient. The fractional contribution of individual species or VOC groups was determined relative to the summed OFP of all species included in the calculation. Species for which MIR coefficients were unavailable were excluded.

2.3 PMF source apportionment

The sources of ambient VOCs were resolved using U.S. EPA PMF 5.0. The observed concentration matrix is expressed as:

$$x_{ij} = \sum_{k=1}^{p} g_{ik} f_{ki} + e_{ij}$$

where x_{ij} is the measured concentration of species j in sample i, g_{ik} represents the contribution of factor k to sample i, f_{kj} is the profile of species j in factor k, and e_{ij} is the model residual. PMF constrains both factor contributions and factor profiles to non-negative values (Liu et al., 2023a; Gu et al., 2022).

Concentration and uncertainty matrices constructed from representative VOC species measured during the 2021-2022 campaigns were used as model inputs. Twenty runs were performed, and the final five-factor solution was selected according to model performance and solution stability.

2.4 WRF-Chem simulations

The WRF-Chem modeling framework followed that used in our previous study(Ye et al., 2025), with the model domain, emission inputs, simulation period, and sensitivity

https://doi.org/10.5194/egusphere-2026-4504
Preprint. Discussion started: 3 September 2026

settings adapted specifically for the summertime O_3 episode in Siping. A 6 km horizontal-resolution domain comprising 150 × 150 grid cells was established over Northeast China and centered at 43.5° N, 124.5° E (Fig. S2). Atmospheric chemistry was represented using the SAPRC-99 mechanism.

Anthropogenic emissions combined the localized Siping emission inventory with the Multi-resolution Emission Inventory for China (MEIC) and were separated into agriculture, industry, power plants, residential combustion, and transportation. Biogenic emissions were calculated online using the Model of Emissions of Gases and Aerosols from Nature (MEGAN). Additional information on the meteorological and chemical configurations is provided in Text S2 and Table S2.

Model performance was assessed using hourly $PM_{2.5}$, O_3, NO_2, SO_2, and CO observations from the National Ambient Air Quality Monitoring Station in Siping. Three statistical metrics were used: mean bias (MB), root mean square error (RMSE), and index of agreement (IOA):

$$MB = \frac{\sum_{i=1}^{N}(P_i - O_i)}{\sum_{i=1}^{N} O_i}$$

$$RMSE = \left[\frac{1}{N}\sum_{i=1}^{N}(P_i - O_i)^2\right]^{\frac{1}{2}}$$

$$IOA = 1 - \frac{\sum_{i=1}^{N}(P_i - O_i)^2}{\sum_{i=1}^{N}(|P_i - \bar{O}| + |O_i - \bar{O}|)^2}$$

where P_i and O_i denote simulated and observed values, respectively, N is the number of paired observations, and $\bar{O}$ represents the mean observed value.

2.5 Sensitivity analysis and EKMA

The factor separation approach (FSA) used to distinguish emission and transport effects followed the modeling framework established in our previous work (Ye et al., 2025), with scenario settings redesigned for summertime O_3 in Siping. The analysis covered 11-18 June 2021. Three sensitivity experiments, together with the baseline simulation, were used to separate the contributions associated with local emissions and regional transport and to quantify their interactions. The corresponding anthropogenic emission configurations are provided in Table S3, while the mathematical formulation of the FSA is described in Text S3.

https://doi.org/10.5194/egusphere-2026-4504
Preprint. Discussion started: 3 September 2026

A second set of sensitivity simulations was conducted to determine the contributions of individual emission sectors. Emissions from agriculture, industry, power plants, residential combustion, transportation, and biogenic sources were modified separately relative to the baseline simulation. The settings for these source-specific experiments are summarized in Table S4.

The EKMA analysis followed the emission-response framework developed in our previous study(Ye et al., 2026b), but used the Siping-specific emission inventory and chemical conditions. Because the analysis was intended to evaluate controllable anthropogenic precursor reductions, BVOC emissions were maintained at their baseline values. anthropogenic VOC (AVOC) and NO_x emissions were independently varied from 0% to 100% of the baseline inventory at intervals of 10%, forming an 11 × 11 matrix of 121 sensitivity simulations. The resulting O_3 response surface was used to identify precursor-sensitivity regimes and the coordinated AVOC-NO_x reduction pathway.

3 Result & Discussion

3.1 VOC composition, temporal characteristics, and OFP in Siping

During the sampling period, the mean ambient VOC concentration in Siping was 42.33 ± 3.12 ppbv, which was higher than those reported for several other northern Chinese cities, including Qingdao (18.8 ppbv, 2021), Shijiazhuang (29.3 ppbv, 2022), and Zhumadian (17.7 ppbv, 2020) (Wu et al., 2024). The six VOC groups ranked, in descending order of concentration, as follows: alkane (15.65 ppbv), OVOC (13.32 ppbv), halocarbons (5.64 ppbv), alkene (4.50 ppbv), aromatics (2.80 ppbv), and alkyne (1.02 ppbv). Alkanes were the dominant group, accounting for 36.98% of total VOCs, followed by OVOCs, which contributed 31.48%. Alkenes and halocarbons exhibited comparable abundances, whereas aromatics and alkynes contributed relatively little to the total VOC burden.

The concentrations of individual VOC species are summarized in Table S6. Isopentane was the most abundant species, with a concentration of 29.14 ppbv, followed by acetone, n-pentane, isobutane, n-butane, propane, ethane, ethylene, and acetylene. A comparison of key VOC species between the summer of 2021 and 2022 is presented in Table S7. The dominant VOC species and their rankings showed little

https://doi.org/10.5194/egusphere-2026-4504
Preprint. Discussion started: 3 September 2026

interannual variation, with C_4-C_5 alkanes, acetone, and short-chain alkanes consistently accounting for the largest fractions. This consistency suggests that the major emission sources and their relative contributions remained broadly stable during the study period. However, the overall VOC concentration was substantially higher in the summer of 2022 than in 2021. Notably, the concentration of isopentane increased to approximately seven times that measured during the same period in the previous year, indicating that this species warrants particular attention.

Figure 1 illustrates the diurnal variations in VOC composition in Siping. The VOC concentrations consistently exhibited distinct morning and evening peaks, a pattern that agrees well with observations reported for other Chinese cities, such as Jinan in Shandong Province during summer (Liu et al., 2023b) and Weinan in Shaanxi Province (Li et al., 2022a). This consistency suggests that the diurnal variation of VOCs in AUI remains primarily controlled by vehicular emissions, reflecting a common emission and photochemistry-driven pattern across regions. Analysis of individual VOC groups further showed that alkane, alkene, and alkyne concentrations during the evening peak were substantially higher than those observed at other times of the day. This increase was likely associated with emission sources exhibiting pronounced temporal patterns, particularly vehicle exhaust and residential biomass combustion (Fuchs et al., 2017).

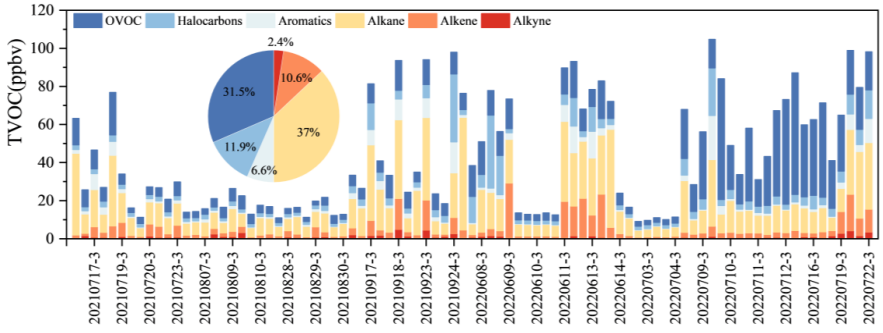

Figure 1: Temporal variations and chemical composition of VOCs in Siping during the summers of 2021-2022.

Building on these results, the OFP of ambient VOCs in Siping was evaluated using the MIR method and compared with the observed O_3 concentrations (Fig. 2). Alkenes

https://doi.org/10.5194/egusphere-2026-4504
Preprint. Discussion started: 3 September 2026

contributed the largest fraction of OFP (51.96%), followed by alkanes (25.02%), OVOCs (11.69%), and aromatics (10.78%), whereas halocarbons (0.55%) and alkynes (0.0009%) made only minor contributions. This distribution differs substantially from the VOC composition, indicating that OFP is determined not only by VOC abundance but also by the intrinsic reactivity of individual species. Further analysis of the major contributors to OFP (Table S8) showed that ethylene, propylene, and isoprene were the dominant alkene species driving O_3 formation. These compounds consistently ranked among the largest contributors to OFP across different sampling months in both 2021 and 2022. Consequently, alkenes became the largest contributor to OFP despite their relatively low ambient concentrations. Notably, during the warmer months (August 2021 and July 2022), isoprene ranked among the top three contributors to OFP across all VOC species, highlighting the critical role of BVOCs in summertime O_3 formation. Among alkanes, isopentane, n-butane, propane, and ethane contributed most to OFP, primarily because of their relatively high ambient concentrations.

The diurnal variation in OFP closely followed that of VOC concentrations, with pronounced morning and evening peaks. Table S9 lists the top 10 VOC species contributing to OFP during the morning, afternoon, and evening periods. During the morning peak, isopentane, isobutane, n-pentane, and acetone were the largest contributors to OFP. The dominant contribution of alkanes indicates that vehicular emissions during the morning rush hour were an important driver of O_3 formation (Yang et al., 2019). During the afternoon, ethylene and acetone became the major contributors to OFP. As an important secondary oxidation product, the elevated contribution of acetone suggests that atmospheric oxidation had reached its maximum intensity. At this stage, substantial consumption of VOCs by photochemical reactions led to an overall decline in OFP (Li et al., 2022a; Sha et al., 2021). Notably, as a representative AUI, Siping experiences substantial BVOC emissions from intensive crop growth and agricultural shelterbelts during summer. The diurnal variation in isoprene OFP first decreased and then increased, reaching its maximum in the evening. This pattern suggests that elevated daytime temperatures suppress plant isoprene

https://doi.org/10.5194/egusphere-2026-4504
Preprint. Discussion started: 3 September 2026

emissions, followed by compensatory emissions later in the day (Li et al., 2025); Despite the reduction in absolute emissions, isoprene remained one of the leading contributors to OFP during the afternoon because of its high chemical reactivity and the concurrent depletion of anthropogenic VOCs by photochemical oxidation (Tan et al., 2021). These findings further confirm the important role of BVOCs, particularly isoprene, in O_3 formation in Siping and underscore the necessity of jointly considering natural and anthropogenic emissions when developing O_3 control strategies for agricultural regions.

During the evening, the contributions of C_4-C_5 alkenes to OFP increased markedly, particularly those of trans-2-pentene and trans-2-butene. These species are strongly associated with natural gas, coal gas, and solid fuel combustion, suggesting that residential emissions from the surrounding areas substantially influenced ambient VOC levels (Li et al., 2022b; Gao et al., 2021). It is worth noting that the temporal trend of OFP did not correspond to the observed variation in O_3 concentrations (Fig. 2), further demonstrating the complex nonlinear relationship between VOCs and O_3 formation in Siping. Therefore, source apportionment and numerical modeling are required to further elucidate the underlying mechanisms.

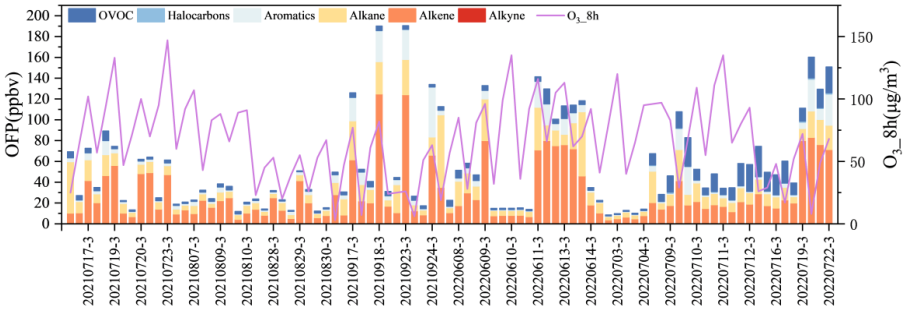

Figure 2: Temporal variations in OFP of VOCs and observed O_3 concentrations in Siping during the summers of 2021-2022.

3.2 Source apportionment of VOCs

To identify the sources of ambient VOCs in Siping, PMF analysis was performed using representative VOC species collected during the 2021-2022 sampling

https://doi.org/10.5194/egusphere-2026-4504
Preprint. Discussion started: 3 September 2026

campaigns. The identified source profiles and their relative contributions are presented in Fig. 3. Based on the monitoring data, together with the local emission inventory and PMF source profiles, VOC emissions in Siping were classified into five major source categories: vehicle emission, industrial combustion, solvent source, gaseous fuel combustion, and biogenic source.

A detailed interpretation of the PMF factors is provided in Text S4. Factor 1 was characterized by high loadings of aromatic compounds and several halocarbons, including styrene, ethylbenzene, xylenes, ethyl acetate, and chloroform. This factor was therefore identified as solvent source (Li et al., 2024; Sha et al., 2021; Wang et al., 2023b). Factor 2 was dominated by light hydrocarbons, together with chlorofluorocarbons and methyl tert-butyl ether (MTBE), indicating a mixed source associated with gaseous fuel use, combustion processes, and refrigerant emissions. Accordingly, this factor was attributed to gaseous fuel combustion, including natural gas and liquefied petroleum gas (LPG) (Zhu et al., 2025; Man et al., 2020; Wu et al., 2023a). Factor 3 exhibited exceptionally high isoprene together with abundant oxygenated VOCs, indicating a secondary/biogenic source dominated by biogenic emissions (Wang et al., 2024; Vestenius et al., 2021; Wu et al., 2023b). Factor 4 was characterized by substantial contributions from C_4-C_6 alkanes and alkenes, including isopentane, n-pentane, n-butane, ethylene, and cis-2-butene, as well as elevated toluene, which are typical tracers of vehicle emissions (Zhou et al., 2020; Man et al., 2020; Sun et al., 2021; Zi et al., 2023). Factor 5 was enriched in heavier aromatic compounds, such as trimethylbenzene and diethyl benzene, together with long-chain alkanes, and was therefore identified as industrial combustion, primarily associated with diesel-related heavy-oil combustion (Frischmon and Hannigan, 2024; Liang et al., 2020; Lyu et al., 2021).

Fig. 3(b) presents the relative contributions of different VOC emission sources in Siping during the 2021-2022 sampling period based on the PMF results. Vehicle emissions were the dominant source, accounting for 56.4% of total VOCs. Gaseous fuel combustion and solvent source contributed 15.1% and 13.3%, respectively. Biogenic sources accounted for 8.8%, likely reflecting the strong influence of

https://doi.org/10.5194/egusphere-2026-4504
Preprint. Discussion started: 3 September 2026

agricultural activities in Siping, whereas industrial combustion contributed only 6.4%. Notably, the contribution of vehicle emissions in Siping was substantially higher than those reported for other cities and background sites, including Qingdao (17.1%) (Wu et al., 2023a), Deqing, Zhejiang (11.8%) (Wang et al., 2026), the Shangdianzi regional background station (23.4%; 40.65°N, 117.12°E), which is located at a similar latitude and is part of the Global Atmosphere Watch (GAW) network (Han et al., 2021), and Harbin (28.9%; 45°45′N, 126°41'E), another city at a comparable latitude (Xuan et al., 2021). The exceptionally high contribution of vehicle emissions suggests that, in AUI, where industrial sources are relatively limited, seasonal BVOC emissions together with urban and transit traffic constitute the dominant local precursor sources. This unique emission structure likely leads to O_3 formation efficiency and precursor sensitivity that differ fundamentally from those observed in large industrialized cities, highlighting the need for integrated analyses combining receptor models and chemical transport modeling to elucidate the mechanisms.

https://doi.org/10.5194/egusphere-2026-4504
Preprint. Discussion started: 3 September 2026

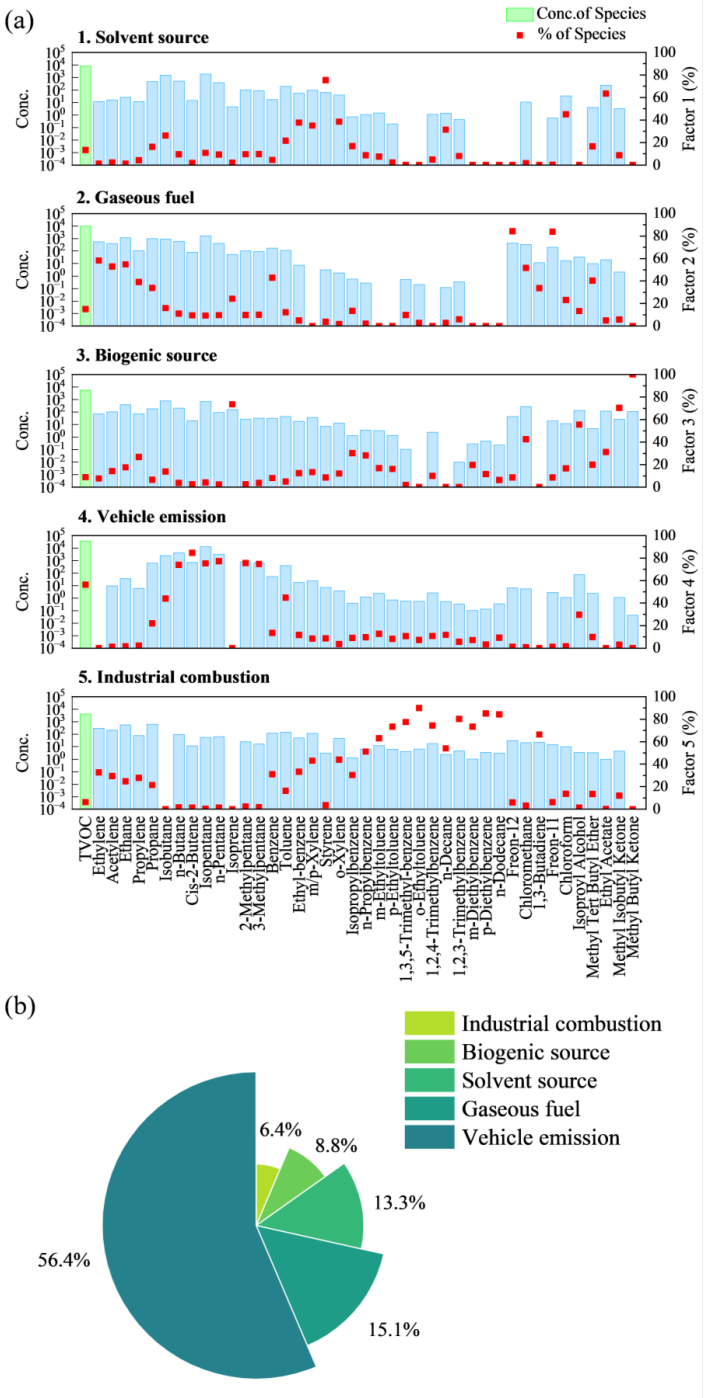

355

356 Figure 3: PMF-resolved factor contribution characteristics and source contributions

https://doi.org/10.5194/egusphere-2026-4504
Preprint. Discussion started: 3 September 2026

3.3 WRF-Chem model evaluation

3.3.1 Evaluation of summertime O_3 simulations

The WRF-Chem simulations covered the period from 11 to 18 June 2021. Fig.S3 compares the observed and simulated hourly O_3 concentrations at the National Ambient Air Quality Monitoring Stations in Jilin Province and Siping during the simulation period. Relative to the observations, the model slightly overestimated O_3 concentrations across Jilin Province. Nevertheless, the simulated O_3 exhibited good agreement with the observations, with IOA values of 0.84 and 0.87 for Jilin Province and Siping, respectively. More importantly, the model successfully reproduced the overall diurnal variation in O_3 concentrations. For Siping, the MB of the simulated hourly O_3 concentration was -4.2 $\mu g/m^3$, these results indicate that the model reasonably captured the temporal evolution of hourly O_3 concentrations during the study period.

Fig.S4 presents the spatial distributions of the simulated and observed mean near-surface concentrations of the maximum daily 8 h average (MDA8) O_3 and other major air pollutants during 11-18 June 2021. The model successfully reproduced the spatial distribution of major air pollutants over Siping and the surrounding region. The simulated mean MDA8 O_3 concentrations ranged from 125 to 175 $\mu g/m^3$, corresponding to a slight pollution level. Meanwhile, the observed mean MDA8 O_3 concentration at the monitoring site was 162.63 $\mu g/m^3$, while the simulated values exhibited a slight underestimation compared to the observation.

Overall, the WRF-Chem model satisfactorily reproduced both the temporal variations and spatial distributions of major air pollutants over Jilin Province and Siping. However, discrepancies between the simulations and observations remained. In addition to uncertainties associated with meteorological simulations, such as planetary boundary layer development and horizontal wind fields, uncertainties in anthropogenic emission inventories are considered a major source of model bias (Ye et al., 2025).

3.3.2 Contributions of background concentrations, local emissions, and regional transport to MDA8 O_3

Figure S5 illustrates the spatial distributions of background MDA8 O_3 concentrations, locally produced MDA8 O_3, and MDA8 O_3 associated with regional transport in Siping and the surrounding areas during 11-18 June 2021. Background concentrations

https://doi.org/10.5194/egusphere-2026-4504
Preprint. Discussion started: 3 September 2026

accounted for more than 50% of the total MDA8 O_3 burden, contributing approximately 80-100 μg/m^3. In contrast, the contribution from local emissions was relatively small, averaging about 15 μg/m^3 (approximately 10% of total MDA8 O_3) and was primarily concentrated in the Tiedong and Tiexi districts. Regional transport also made a substantial contribution, ranging from 40 to 50 μg/m^3 (approximately 30-40% of total MDA8 O_3). As shown by the wind field in Fig. S5(c), southwesterly winds prevailed over Northeast China during summer. On a broader regional scale, the southwestern upwind region is characterized by higher total column O_3. Consequently, atmospheric disturbances originating from the southwest can reshape regional circulation patterns, causing O_3 pollution in Siping to be strongly influenced by elevated background O_3 transported from this direction (Du et al., 2026; Shi et al., 2024).

The quantitative contributions of background concentrations, local emissions, and regional transport to MDA8 O_3 in Siping are summarized in Table S10. The mean MDA8 O_3 concentration was 155.04 μg/m^3, of which the background concentration contributed 88.79 μg/m^3 (57.27%) in Siping. Regional transport represented the second largest contributor, accounting for 49.89 μg/m^3 (32.18%). By comparison, MDA8 O_3 produced from local emissions contributed only 15.71 μg/m^3 (10.13%). Interactions among atmospheric pollutants slightly increased the O_3 concentration by 0.65 μg/m^3 (0.42%), indicating a weak net chemical production. These results are generally consistent with the observed pollution characteristics.

Overall, background concentrations and regional transport together accounted for nearly 90% of the total MDA8 O_3 concentration, highlighting the dominant influence of regional processes on summertime MDA8 O_3 pollution in Siping. This strong dependence on regional transport substantially limits the effectiveness of strategies based solely on local emission reductions. Therefore, optimizing O_3 mitigation in AUI requires integrating regional emission control with analyses of the nonlinear relationship between MDA8 O_3 and precursor response surface (e.g., EKMA) and detailed emission inventories to identify the most effective control pathways.

3.3.3 Contributions of major emission sources to summertime O_3 in Siping

Figure 4 and Fig. S6 present the spatial distributions of the mean contributions and percentage contributions of industrial, power plant, residential, transportation, agricultural, and biogenic sources to MDA8 O_3 concentrations in Siping during 11-18

https://doi.org/10.5194/egusphere-2026-4504
Preprint. Discussion started: 3 September 2026

June 2021. The quantitative contributions of these source categories are summarized in Table 1. Among all sources, biogenic emissions made the largest contribution to O_3, accounting for 11.76% (18.24 μg/m^3) of the total concentration. Although biogenic emissions were one of the dominant contributors, their contribution was comparable to or lower than those reported for other AUI and temperate regions, including agricultural and forested areas in six U.S. cities (10–19%) (Zhang et al., 2017) , the Yangtze River Delta (9.5–20%) (Li et al., 2019), the North China Plain (29.5%), the Pearl River Delta (24.7%), and India (15.0%) (Gao et al., 2020). This relatively modest contribution is primarily attributable to the land-use characteristics surrounding Siping. The region is dominated by cropland, where BVOC emissions are generally lower than those from forest ecosystems. Moreover, vegetation with high isoprene and monoterpene emission capacities occupies only a limited area, restricting the regional BVOC emission potential (Li et al., 2025). Therefore, despite being a representative AUI, Siping does not exhibit an exceptionally strong biogenic enhancement of O_3 formation compared with other regions.

Industrial emissions and transportation were the second and third largest contributors, accounting for 11.19% (17.35 μg/m^3) and 10.87% (16.85 μg/m^3), respectively. In contrast, contributions from power plants, residential combustion, and agricultural emissions were relatively small, at 1.14%, 1.84%, and 0.92%, respectively. Notably, agricultural emissions contributed only 0.92% to MDA8 O_3, substantially less than other anthropogenic sources. This result is mainly because agricultural emissions in the present emission inventory are dominated by NH_3 released from agricultural activities. NH_3 primarily promotes the formation of secondary inorganic aerosols through atmospheric acid-base reactions and has only a limited direct influence on O_3 photochemistry (Pan et al., 2024). Overall, these results indicate that industrial emissions, biogenic emissions, and transportation were the primary drivers of summertime MDA8 O_3 pollution in Siping.

A notable finding is the discrepancy between the PMF and WRF-Chem results. PMF analysis showed that vehicle emissions accounted for 56.4% of total VOC concentrations, making them the dominant VOC source. In contrast, WRF-Chem sensitivity simulations indicated that transportation contributed only 10.87% to summertime MDA8 O_3. This contrast between a high contribution to VOCs and a relatively low contribution to MDA8 O_3 further highlights the strong nonlinearity between precursor emissions and O_3 formation in AUI.

https://doi.org/10.5194/egusphere-2026-4504
Preprint. Discussion started: 3 September 2026

Several factors explain this discrepancy. First, background concentrations and regional transport together accounted for nearly 90% of the total O_3 concentration, substantially diluting the incremental O_3 produced by local transportation emissions and limiting their contribution to ambient O_3. Second, although transportation emits large amounts of VOCs, these emissions are dominated by C_4-C_5 alkanes and some aromatic compounds. In contrast, the OFP analysis demonstrated that O_3 formation in Siping is more strongly controlled by highly reactive species, particularly alkenes such as ethylene, propylene, and isoprene. Despite their relatively small contribution to total VOC concentrations, BVOCs, especially isoprene, exhibit exceptionally high chemical reactivity. Under strong summertime solar radiation, they efficiently enhance RO_x radical cycling and substantially increase O_3 production efficiency. These findings indicate that O_3 formation depends more strongly on the abundance of highly reactive precursors than on total VOC concentrations alone. Therefore, inferring O_3 formation directly from VOC concentrations or source contributions may lead to substantial bias in AUI. Integrating high-resolution WRF-Chem simulations with the EKMA provides a more robust framework for identifying effective O_3 control strategies.

https://doi.org/10.5194/egusphere-2026-4504
Preprint. Discussion started: 3 September 2026

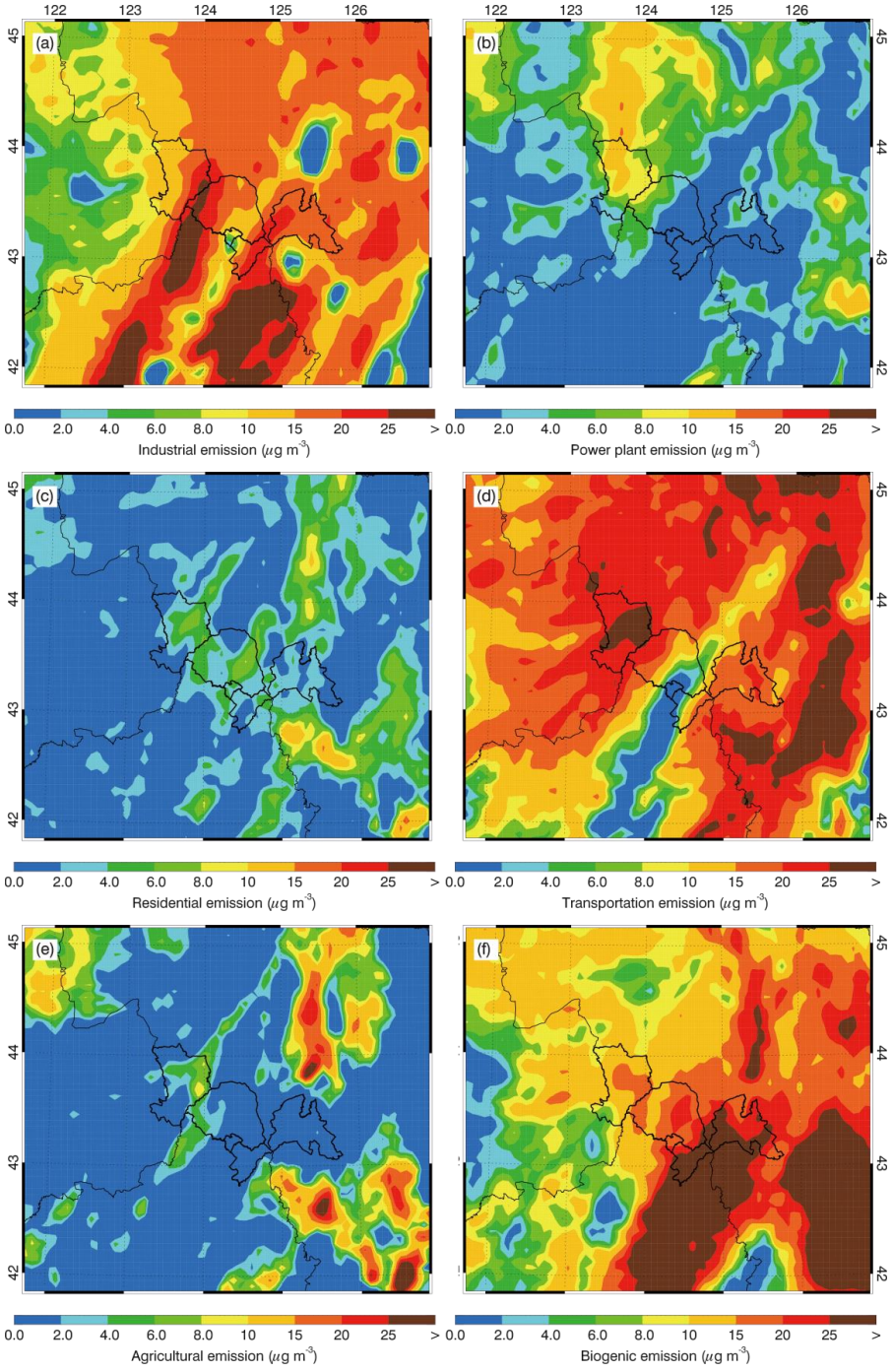

Figure 4. Spatial distributions of the mean contributions of industrial, power plant, residential, transportation, agricultural, and biogenic sources to MDA8 O_3 concentrations in Siping during 11-18 June 2021.

https://doi.org/10.5194/egusphere-2026-4504
Preprint. Discussion started: 3 September 2026

Table 1: Contributions of major emission sources in Northeast China to MDA8 O_3 concentrations in Siping during the simulation period.

Case	MDA8 O_3	
	Concentration（μg/m^3）	Contribution（%）
Baseline simulation	155.04	/
Industrial emissions	17.35	11.19
Power plant emissions	1.77	1.14
Residential emissions	2.85	1.84
Transportation emissions	16.85	10.87
Agricultural emissions	1.43	0.92
Biogenic emissions	18.24	11.76

3.3.4 Sensitivity analysis of summertime O_3 formation and control strategies

To further investigate the sensitivity of summertime O_3 formation in Siping, EKMA isopleths were constructed by varying AVOC and NO_x emissions (Fig. 5(a)). The inflection points of the O_3 isopleths were connected to derive the ridgeline, along which the AVOC/NO_x ratio was approximately 4:1, representing the most effective coordinated reduction pathway. The ridgeline separated the EKMA diagram into different sensitivity regimes, with the reference condition of Siping located close to this boundary. Given the relatively low AVOC emissions, no distinct VOC-limited regime was identified; instead, summertime O_3 formation occurred within a transition regime where both AVOCs and NO_x influenced ozone production. Under this condition, coordinated precursor controls are required to achieve effective O_3 mitigation, while the actual reduction efficiency may further depend on the emission sources contributing to these precursors.

However, the relationship between precursor emissions and O_3 formation is more complex in an AUI than in conventional urban environments because anthropogenic emissions coexist with biogenic VOC inputs and substantial regional background ozone. Therefore, control strategies based solely on bulk VOC or NO_x reductions may not fully capture the ozone mitigation potential of individual emission sectors.

To identify the most effective controllable sources under this complex chemical

https://doi.org/10.5194/egusphere-2026-4504
Preprint. Discussion started: 3 September 2026

environment, combining the source apportionment and sensitivity simulations, this study identified biogenic, industrial, and transportation emissions as the major precursor sources of summertime O_3 in Siping. According to the 2021 local emission inventory, regional BVOCs are emitted predominantly by crops and natural vegetation and therefore represent an uncontrollable natural source. This characteristic is a common challenge for O_3 mitigation in AUI across northern China (Ye et al., 2025). Consequently, emission control efforts in Siping should focus primarily on anthropogenic sources, particularly industry and transportation.

Our previous studies have demonstrated that emission-inventory-based mitigation scenarios provide an effective framework for evaluating ozone reduction potential (Ye et al., 2026a). Therefore, we further combined EKMA analysis with emission inventory reductions to quantify the ozone mitigation effectiveness of the three major emission sources. Nine emission reduction scenarios were designed to evaluate the effectiveness of different control strategies (Fig. 5(b)-(d) and Table S11). The results reveal clear differences in O_3 mitigation efficiency between industrial and transportation emissions. For industrial process emissions (Industry 1), the VOC/ NO_x emission ratio was close to 1:1, placing the system near the NO_x-limited regime. However, because VOC emissions from this source were relatively low, reducing these emissions alone produced only a limited decrease in O_3, with a maximum reduction of 0.9% even under a 100% emission reduction scenario. Industrial fossil fuel combustion (Industry 2) exhibited an even lower VOC/NO_x ratio, deviating further from the optimal EKMA control pathway and resulting in relatively poor O_3 mitigation efficiency. These findings suggest that reducing emissions from individual industrial sectors alone is insufficient to effectively alleviate O_3 pollution in Siping, a limitation that may also apply to other AUI.

In contrast, transportation emissions exhibited substantially greater mitigation potential. As the dominant source of VOCs in Siping, transportation represents the most effective controllable target for O_3 reduction. Scenario simulations showed that reducing transportation emissions by 50% and 100% decreased the mean O_3 concentration from 125 $\mu g/m^3$ to 121 $\mu g/m^3$ and 114 $\mu g/m^3$, corresponding to reductions of 3.2% and 8.8%, respectively. These results are consistent with the source contribution analysis (Table 1), confirming that transportation emission control is the most effective and practically achievable strategy for mitigating summertime O_3 pollution in Siping.

https://doi.org/10.5194/egusphere-2026-4504
Preprint. Discussion started: 3 September 2026

From the perspective of O_3 control effectiveness, these findings also highlight the environmental benefits of transportation electrification. For AUI such as Siping, replacing conventional vehicles with electric vehicles can directly reduce emissions from the dominant controllable precursor source, providing an efficient and practical pathway for O_3 mitigation. These results provide scientific evidence to support coordinated O_3 management and green transportation policies in AUI and offer useful guidance for developing integrated precursor control strategies in agricultural-urban regions.

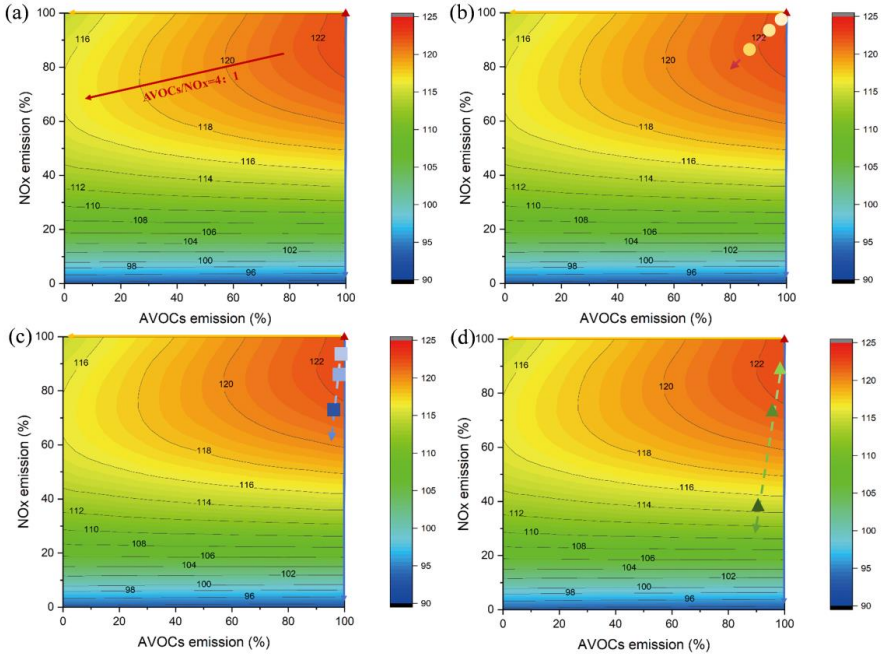

Figure 5: EKMA isopleths of summertime O_3 (MDA8 O_3) in Siping. (a) EKMA isopleths under the baseline emission scenario. (b) Emission reduction scenarios for industrial process emissions (Industry 1). (c) Emission reduction scenarios for industrial fossil fuel combustion (Industry 2). (d) Emission reduction scenarios for vehicle emissions. The x- and y-axes represent the fractions of remaining AVOC and NO_x emissions relative to the baseline emissions, respectively. The red triangle in the upper-right corner denotes the baseline emission scenario (100% AVOC and 100% NO_x emissions). The circles, squares, and triangles represent the emission reduction scenarios for Industry 1, Industry 2, and vehicle emissions, respectively. Marker colors from light to dark indicate emission reductions of 20%, 50%, and 100%, respectively.

https://doi.org/10.5194/egusphere-2026-4504
Preprint. Discussion started: 3 September 2026

4 Conclusions

This study investigated Siping, a representative AUI in Northeast China, by integrating VOC observations, PMF source apportionment, WRF-Chem simulations, and EKMA analysis to elucidate the interplay between local emissions and regional processes in summertime O_3 pollution. PMF results showed that vehicle emissions were the dominant local VOC source, accounting for 56.4% of total VOCs. In contrast, WRF-Chem simulations indicated that background O_3 and regional transport together contributed nearly 90% of ambient O_3, highlighting the strong influence of regional-scale processes on O_3 levels in the AUI. Notably, despite this dominant regional influence, reductions in transportation emissions still effectively decreased O_3 concentrations. This finding demonstrates that the dominance of regional processes does not imply that local emission control is ineffective, and that the mitigation potential of a local source cannot be evaluated solely from its contribution to the existing O_3 burden.

Several limitations should be acknowledged. VOC measurements were conducted at only one urban site and were restricted to relatively short sampling periods during summer, limiting the representation of spatial heterogeneity within the AUI and seasonal variability in O_3 formation. In addition, the WRF-Chem source attribution and emission-reduction analyses focused on a single representative summertime O_3 episode and were subject to uncertainties in meteorological fields and emission inventories. In particular, the predicted O_3 responses to hypothetical emission-reduction scenarios cannot be directly validated through equivalent emission perturbations in the real atmosphere. Future studies combining multi-site, multi-season, and long-term continuous observations are therefore needed to further assess the robustness and broader applicability of the mechanisms identified here.

More importantly, this study provides broader atmospheric-chemistry implications for understanding O_3 formation and control in AUIs. Many AUIs worldwide lack major industrial point sources but are simultaneously influenced by anthropogenic emissions such as traffic, agricultural and vegetation-related biogenic emissions, and substantial regional O_3 background and transport. Despite its pronounced AUI characteristics, the biogenic contribution remains lower than that reported for forest regions, indicating that an agriculture-dominated landscape does not necessarily translate into a disproportionately large biogenic O_3 contribution. Under such conditions, the largest

https://doi.org/10.5194/egusphere-2026-4504
Preprint. Discussion started: 3 September 2026

local precursor source does not necessarily correspond to the largest contributor to ambient O_3, while a source making only a modest contribution to the existing O_3 burden may still have considerable mitigation potential. Our results show that transportation emission reductions remain effective even when background O_3 and regional transport account for nearly 90% of ambient O_3. This effectiveness arises because transportation simultaneously emits both VOCs and NO_x, and their coordinated reduction shifts the precursor mixture along a more favorable pathway for O_3 mitigation identified by the EKMA response surface. In contrast, reductions in some industrial sources produce only limited O_3 benefits because of their less favorable VOC/NO_x emission ratios. Therefore, O_3 control in AUIs should not be prioritized solely according to the source contributions to ambient O_3, but should also consider precursor reactivity, source-specific VOC/NO_x emission structures, and nonlinear photochemical sensitivity. This perspective links regional transport, local emission characteristics, and nonlinear O_3 chemistry, and demonstrates that targeted control of local anthropogenic sources with favorable precursor-reduction characteristics can remain effective even when regional processes dominate the overall O_3 burden. With the continuing electrification of the vehicle fleet, coordinated reductions in traffic-related VOC and NO_x emissions are becoming an increasingly feasible local intervention and may provide additional co-benefits for O_3 mitigation in AUIs. Accordingly, for AUIs characterized by strong regional O_3 backgrounds, intensive mixing of anthropogenic and biogenic precursors, and pronounced agricultural-urban transitions, combining regional cooperative control with targeted reductions in key local precursors may be more effective than control strategies based solely on local source contributions.

Data availability

The data of this paper can be obtained from Zenodo (https://doi.org/10.5281/zenodo.21532281)

Author contributions

Xinpeng Ye: Writing (Original draft preparation), Data curation. **Qian Jiang:** Methodology. Validation. **Jin Ban:** Methodology. **Mengyu Xie:** Validation. **Qianyi**

https://doi.org/10.5194/egusphere-2026-4504
Preprint. Discussion started: 3 September 2026

Xu: Methodology. **Zeyu Wang:** Investigation. **Jian Sun:** Funding acquisition. Writing (Review & Editing), Supervision. **Hongai Zhang:** Methodology. **Xinyi Niu:** Funding acquisition. **Hongmei Xu:** Methodology. **Zhenxing Shen:** Conceptualization, Supervision. **Guohui Li:** Methodology. Supervision.

Competing interests

The authors declare that none of the authors has any competing interests.

Acknowledgments

This research was supported by the Natural Science Foundation of Shaanxi Province (2026JC-YXQN-117), the Natural Science Foundation of China (Grant No. 42207117).

References

Benka-Coker, W., Hoskovec, L., Severson, R., Balmes, J., Wilson, A., and Magzamen, S.: The joint effect of ambient air pollution and agricultural pesticide exposures on lung function among children with asthma, Environmental Research, 190, 109903, https://doi.org/10.1016/j.envres.2020.109903, 2020.

Cao, J., Situ, S., Hao, Y., Xie, S., and Li, L.: Enhanced summertime ozone and SOA from biogenic volatile organic compound (BVOC) emissions due to vegetation biomass variability during 1981–2018 in China, Atmos. Chem. Phys., 22, 2351-2364, 10.5194/acp-22-2351-2022, 2022.

Carter, W. P. L.: Development of Ozone Reactivity Scales for Volatile Organic Compounds, Air & Waste, 44, 881-899, 10.1080/1073161X.1994.10467290, 1994.

Du, Y., Yang, F., Lou, S., Lyu, B., Huang, R., Shi, G., Hu, Y., Jiang, Y., and Wang, N.: The Role of Chemical Boundary Conditions in Simulating Summer Ozone and Cross-Boundary Transport over China, EGUsphere, 2026, 1-30, 2026.

Frischmon, C. and Hannigan, M.: VOC source apportionment: How monitoring characteristics influence positive matrix factorization (PMF) solutions, Atmospheric Environment: X, 21, 100230, https://doi.org/10.1016/j.aeaoa.2023.100230, 2024.

Fuchs, H., Tan, Z., Lu, K., Bohn, B., Broch, S., Brown, S. S., Dong, H., Gomm, S., Häseler, R., He, L., Hofzumahaus, A., Holland, F., Li, X., Liu, Y., Lu, S., Min, K. E., Rohrer, F., Shao, M., Wang, B., Wang, M., Wu, Y., Zeng, L., Zhang, Y., Wahner, A., and Zhang, Y.: OH reactivity at a rural site (Wangdu) in the North China Plain: contributions from OH reactants and experimental OH budget, Atmos. Chem. Phys., 17, 645-661, 10.5194/acp-17-645-2017, 2017.

Gao, M., Gao, J. H., Zhu, B., Kumar, R., Lu, X., Song, S. J., Zhang, Y. Z., Jia, B. X., Wang, P., Beig, G. R., Hu, J. L., Ying, Q., Zhang, H. L., Sherman, P., and McElroy, M. B.: Ozone pollution over China and India: seasonality and sources, ATMOSPHERIC CHEMISTRY AND PHYSICS, 20, 4399-4414, 10.5194/acp-20-4399-2020, 2020.

https://doi.org/10.5194/egusphere-2026-4504
Preprint. Discussion started: 3 September 2026

Gao, Y., Li, M., Wan, X., Zhao, X., Wu, Y., Liu, X., and Li, X.: Important contributions of alkenes and aromatics to VOCs emissions, chemistry and secondary pollutants formation at an industrial site of central eastern China, Atmospheric Environment, 244, 117927, https://doi.org/10.1016/j.atmosenv.2020.117927, 2021.

Gu, Y., Liu, B., Dai, Q., Zhang, Y., Zhou, M., Feng, Y., and Hopke, P. K.: Multiply improved positive matrix factorization for source apportionment of volatile organic compounds during the COVID-19 shutdown in Tianjin, China, Environment International, 158, 106979, https://doi.org/10.1016/j.envint.2021.106979, 2022.

Gupta, P., Payra, S., Bhatla, R., and Verma, S.: WRF-Chem modeling study of heat wave driven ozone over southeast region, India, Environmental Pollution, 340, 122744, https://doi.org/10.1016/j.envpol.2023.122744, 2024.

Han, T., Ma, Z., Li, Y., Pu, W., Wu, J., Li, Z., Shang, J., He, D., Zhou, L., and Wang, Y.: Chemical characteristics and source apportionments of volatile organic compounds (VOCs) before and during the heating season at a regional background site in the North China Plain, Atmospheric Research, 262, 105778, https://doi.org/10.1016/j.atmosres.2021.105778, 2021.

Li, J., Deng, S., Li, G., Lu, Z., Song, H., Gao, J., Sun, Z., and Xu, K.: VOCs characteristics and their ozone and SOA formation potentials in autumn and winter at Weinan, China, Environmental Research, 203, 111821, https://doi.org/10.1016/j.envres.2021.111821, 2022a.

Li, J., Deng, S., Tohti, A., Li, G., Yi, X., Lu, Z., Liu, J., and Zhang, S.: Spatial characteristics of VOCs and their ozone and secondary organic aerosol formation potentials in autumn and winter in the Guanzhong Plain, China, Environmental Research, 211, 113036, https://doi.org/10.1016/j.envres.2022.113036, 2022b.

Li, L., An, J., Huang, L., Yan, R., Huang, C., and Yarwood, G.: Ozone source apportionment over the Yangtze River Delta region, China: Investigation of regional transport, sectoral contributions and seasonal differences, Atmospheric Environment, 202, 269-280, https://doi.org/10.1016/j.atmosenv.2019.01.028, 2019.

Li, R., Xia, Z., You, B., Shi, B., and Fu, J.: Volatile Organic Compound Emission Inventory for Pesticide Spraying in an Agricultural City of Northeast China: Real-Time Monitoring and Method Optimization, Agriculture, 14, 1223, 2024.

Li, S., Yuan, X., Li, S., Zhou, Y., Wang, S., Zhang, K., Agathokleous, E., Blande, J. D., and Feng, Z.: Extreme Heat Event Alters BVOC Responses to Elevated Ozone: From Physiology to Emission Patterns, Environmental Science & Technology, 59, 12132-12144, 10.1021/acs.est.5c01132, 2025.

Liang, X., Sun, X., Xu, J., and Ye, D.: Improved emissions inventory and VOCs speciation for industrial OFP estimation in China, Science of The Total Environment, 745, 140838, https://doi.org/10.1016/j.scitotenv.2020.140838, 2020.

Liu, B., Yang, Y., Yang, T., Dai, Q., Zhang, Y., Feng, Y., and Hopke, P. K.: Effect of photochemical losses of ambient volatile organic compounds on their source apportionment, Environment International, 172, 107766, https://doi.org/10.1016/j.envint.2023.107766, 2023a.

Liu, Y., Gong, Y., Wang, N., Shi, G., Yang, F., Zhang, Y., and Lu, K.: Photochemical mechanism–dependent ozone formation and precursor sensitivity under varying NO_x conditions, EGUsphere, 2026, 1-33, 10.5194/egusphere-2026-1786, 2026.

Liu, Z., Wang, B., Wang, C., Sun, Y., Zhu, C., Sun, L., Yang, N., Fan, G., Sun, X., Xia, Z., Pan, G., Zhu, C., Gai, Y., Wang, X., Xiao, Y., Yan, G., and Xu, C.: Characterization of photochemical losses of volatile organic compounds and their implications for ozone formation potential and source

https://doi.org/10.5194/egusphere-2026-4504
Preprint. Discussion started: 3 September 2026

apportionment during summer in suburban Jinan, China, Environmental Research, 238, 117158, https://doi.org/10.1016/j.envres.2023.117158, 2023b.

Lyu, C., Capps, S. L., Kurashima, K., Henze, D. K., Pierce, G., Hakami, A., Zhao, S., Resler, J., Carmichael, G. R., Sandu, A., Russell, A. G., Chai, T., and Milford, J.: Evaluating oil and gas contributions to ambient nonmethane hydrocarbon mixing ratios and ozone-related metrics in the Colorado Front Range, Atmospheric Environment, 246, 118113, https://doi.org/10.1016/j.atmosenv.2020.118113, 2021.

Man, H., Liu, H., Niu, H., Wang, K., Deng, F., Wang, X., Xiao, Q., and Hao, J.: VOCs evaporative emissions from vehicles in China: Species characteristics of different emission processes, Environmental Science and Ecotechnology, 1, 100002, https://doi.org/10.1016/j.ese.2019.100002, 2020.

Manisalidis, I., Stavropoulou, E., Stavropoulos, A., and Bezirtzoglou, E.: Environmental and Health Impacts of Air Pollution: A Review, Frontiers in Public Health, Volume 8 - 2020, 10.3389/fpubh.2020.00014, 2020.

Masui, N., Shiojiri, K., Agathokleous, E., Tani, A., and Koike, T.: Elevated O3 threatens biological communications mediated by plant volatiles: A review focusing on the urban environment, Critical Reviews in Environmental Science and Technology, 53, 1982-2001, 10.1080/10643389.2023.2202105, 2023.

Pan, D., Mauzerall, D. L., Wang, R., Guo, X., Puchalski, M., Guo, Y., Song, S., Tong, D., Sullivan, A. P., Schichtel, B. A., Collett, J. L., and Zondlo, M. A.: Regime shift in secondary inorganic aerosol formation and nitrogen deposition in the rural United States, Nature Geoscience, 17, 617-623, 10.1038/s41561-024-01455-9, 2024.

Sha, Q. e., Zhu, M., Huang, H., Wang, Y., Huang, Z., Zhang, X., Tang, M., Lu, M., Chen, C., Shi, B., Chen, Z., Wu, L., Zhong, Z., Li, C., Xu, Y., Yu, F., Jia, G., Liao, S., Cui, X., Liu, J., and Zheng, J.: A newly integrated dataset of volatile organic compounds (VOCs) source profiles and implications for the future development of VOCs profiles in China, Science of The Total Environment, 793, 148348, https://doi.org/10.1016/j.scitotenv.2021.148348, 2021.

Shi, B., Liu, G., Fu, J., Zhai, S., He, L., Li, R., and Chen, W.: Traceability and policy suggestions for ozone pollution in heavy industrial city in Northeast China, Environmental Science and Pollution Research, 31, 47630-47643, 10.1007/s11356-024-33992-6, 2024.

Sun, L., Zhong, C., Peng, J., Wang, T., Wu, L., Liu, Y., Sun, S., Li, Y., Chen, Q., Song, P., and Mao, H.: Refueling emission of volatile organic compounds from China 6 gasoline vehicles, Science of The Total Environment, 789, 147883, https://doi.org/10.1016/j.scitotenv.2021.147883, 2021.

Tan, Y., Han, S., Chen, Y., Zhang, Z., Li, H., Li, W., Yuan, Q., Li, X., Wang, T., and Lee, S.-c.: Characteristics and source apportionment of volatile organic compounds (VOCs) at a coastal site in Hong Kong, Science of The Total Environment, 777, 146241, https://doi.org/10.1016/j.scitotenv.2021.146241, 2021.

Tao, C., Peng, Y., Zhang, Q., Zhang, Y., Gong, B., Wang, Q., and Wang, W.: Diagnosing ozone–NOx–VOC–aerosol sensitivity and uncovering causes of urban–nonurban discrepancies in Shandong, China, using transformer-based estimations, Atmos. Chem. Phys., 24, 4177-4192, 10.5194/acp-24-4177-2024, 2024.

Vestenius, M., Hopke, P. K., Lehtipalo, K., Petäjä, T., Hakola, H., and Hellén, H.: Assessing volatile organic compound sources in a boreal forest using positive matrix factorization (PMF), Atmospheric Environment, 259, 118503, https://doi.org/10.1016/j.atmosenv.2021.118503, 2021.

https://doi.org/10.5194/egusphere-2026-4504
Preprint. Discussion started: 3 September 2026

Wang, L., Slowik, J. G., Klein, F., Stefenelli, G., Pospisilova, V., Tong, Y., Baltensperger, U., and Prévôt, A. S. H.: Characteristics of oxygenated volatile organic compounds in Zurich, Switzerland: Sources, composition, and implication for secondary aerosol formation, Chemosphere, 368, 143686, https://doi.org/10.1016/j.chemosphere.2024.143686, 2024.

Wang, Q., Ou, X., Wu, C., Yao, S., Huang, S., Zhu, C., Liao, Z., Wang, K., Zhang, S., and Chen, J.: Machine learning-driven PMF modeling for accurate and objective source identification of VOCs, Atmospheric Pollution Research, 17, 102721, https://doi.org/10.1016/j.apr.2025.102721, 2026.

Wang, R., Duan, W., Cheng, S., and Wang, X.: Nonlinear and lagged effects of VOCs on SOA and O3 and multi-model validated control strategy for VOC sources, Science of The Total Environment, 887, 164113, https://doi.org/10.1016/j.scitotenv.2023.164113, 2023a.

Wang, Y., Yang, Y., Yuan, Q., Li, T., Zhou, Y., Zong, L., Wang, M., Xie, Z., Ho, H. C., Gao, M., Tong, S., Lolli, S., and Zhang, L.: Substantially underestimated global health risks of current ozone pollution, Nature Communications, 16, 102, 10.1038/s41467-024-55450-0, 2025.

Wang, Z., Zhang, P., Pan, L., Qian, Y., Li, Z., Li, X., Guo, C., Zhu, X., Xie, Y., and Wei, Y.: Ambient Volatile Organic Compound Characterization, Source Apportionment, and Risk Assessment in Three Megacities of China in 2019, 10.3390/toxics11080651, 2023b.

Wu, Y., Liu, B., Meng, H., Dai, Q., Shi, L., Song, S., Feng, Y., and Hopke, P. K.: Changes in source apportioned VOCs during high O3 periods using initial VOC-concentration-dispersion normalized PMF, Science of The Total Environment, 896, 165182, https://doi.org/10.1016/j.scitotenv.2023.165182, 2023a.

Wu, Y., Liu, B., Meng, H., Wang, F., Li, S., Xu, M., Shi, L., Zhang, S., Feng, Y., and Hopke, P. K.: Unexpected changes in source apportioned results derived from different ambient VOC metrics, Environment International, 190, 108910, https://doi.org/10.1016/j.envint.2024.108910, 2024.

Wu, Y., Fan, X., Liu, Y., Zhang, J., Wang, H., Sun, L., Fang, T., Mao, H., Hu, J., Wu, L., Peng, J., and Wang, S.: Source apportionment of VOCs based on photochemical loss in summer at a suburban site in Beijing, Atmospheric Environment, 293, 119459, https://doi.org/10.1016/j.atmosenv.2022.119459, 2023b.

Xuan, L., Ma, Y., Xing, Y., Meng, Q., Song, J., Chen, T., Wang, H., Wang, P., Zhang, Y., and Gao, P.: Source, temporal variation and health risk of volatile organic compounds (VOCs) from urban traffic in harbin, China, Environmental Pollution, 270, 116074, https://doi.org/10.1016/j.envpol.2020.116074, 2021.

Yang, J., Roth, P., Durbin, T., and Karavalakis, G.: Impacts of gasoline aromatic and ethanol levels on the emissions from GDI vehicles: Part 1. Influence on regulated and gaseous toxic pollutants, Fuel, 252, 799-811, https://doi.org/10.1016/j.fuel.2019.04.143, 2019.

Ye, X., Yang, J., Wang, R., Sun, J., Liu, Z., Chen, Z., Li, G., and Shen, Z.: From sensitivity regimes to policy action: Evaluating EKMA curve effectiveness with WRF-Chem, OBM, and machine learning, Atmospheric Environment, 365, 121689, https://doi.org/10.1016/j.atmosenv.2025.121689, 2026a.

Ye, X., Yang, J., Chen, Z., Liu, G., Sun, J., Jiang, Q., Huang, X., Gao, Y., Niu, X., Xu, H., Li, G., and Shen, Z.: Triangulating residential biomass burning impacts on PM2.5 via PMF, satellite observation-based emission inventory, and WRF-Chem, Environment International, 201, 109580, https://doi.org/10.1016/j.envint.2025.109580, 2025.

Ye, X. P., Yang, J. E., Wang, R. N., Sun, J., Liu, Z. R., Chen, Z. W., Li, G. H., and Shen, Z. X.: From sensitivity regimes to policy action: Evaluating EKMA curve effectiveness with WRF-Chem, OBM, and machine learning, ATMOSPHERIC ENVIRONMENT, 365, 10.1016/j.atmosenv.2025.121689,

https://doi.org/10.5194/egusphere-2026-4504
Preprint. Discussion started: 3 September 2026

2026b.
Zhang, J., Wei, Y., and Fang, Z.: Ozone Pollution: A Major Health Hazard Worldwide, Frontiers in Immunology, Volume 10 - 2019, 10.3389/fimmu.2019.02518, 2019.
Zhang, R., Cohan, A., Pour Biazar, A., and Cohan, D. S.: Source apportionment of biogenic contributions to ozone formation over the United States, Atmospheric Environment, 164, 8-19, https://doi.org/10.1016/j.atmosenv.2017.05.044, 2017.
Zhang, Y., Xue, L., Carter, W. P. L., Pei, C., Chen, T., Mu, J., Wang, Y., Zhang, Q., and Wang, W.: Development of ozone reactivity scales for volatile organic compounds in a Chinese megacity, Atmos. Chem. Phys., 21, 11053-11068, 10.5194/acp-21-11053-2021, 2021.
Zhang, Z., Zhao, X., Deng, C., Man, H., Qi, L., Zhao, J., Luo, Z., Wang, H., Jing, S., He, T., He, K., and Liu, H.: Multiple enhanced PMF framework addressing ambient processing and factor allocation for VOC source apportionment, Journal of Cleaner Production, 540, 147523, https://doi.org/10.1016/j.jclepro.2026.147523, 2026.
Zhao, N., Zhang, H., and Wang, G.: Revealing the nonlinear responses of PM2.5 and O3 to VOC and NOx emissions from various sources in Shandong, China, Journal of Hazardous Materials, 489, 137655, https://doi.org/10.1016/j.jhazmat.2025.137655, 2025.
Zhou, M., Jiang, W., Gao, W., Zhou, B., and Liao, X.: A high spatiotemporal resolution anthropogenic VOC emission inventory for Qingdao City in 2016 and its ozone formation potential analysis, Process Safety and Environmental Protection, 139, 147-160, https://doi.org/10.1016/j.psep.2020.03.040, 2020.
Zhu, J., Xia, S., Niu, H., Xu, J., Wang, Y., Yu, X., Huang, L., Zhang, K., Wang, Y., Zeng, L., Li, Q., and Li, L.: Volatile organic compounds from typical industries in North China Plain: emissions, air pollution contribution, health risks, and policy implications, Environment International, 202, 109673, https://doi.org/10.1016/j.envint.2025.109673, 2025.
Zi, T., Wang, P., Liu, B., Zhou, Y., Shen, X. e., Zhang, L., Lu, Y., Feng, Q., Yang, Y., and Lang, J.: Evaporative emission characteristics of VOCs from in-use light-duty gasoline vehicles, Atmospheric Environment, 312, 120024, https://doi.org/10.1016/j.atmosenv.2023.120024, 2023.